First-principles study of noble gas impurities and defects in UO_2

Alexander E. Thompson* and C. Wolverton

Department of Materials Science and Engineering, Northwestern University, Evanston, Illinois 60208, USA

(Received 13 March 2011; revised manuscript received 9 September 2011; published 21 October 2011)

We performed a series of density functional theory + U (DFT + U) calculations to explore the energetics of various defects in UO_2, i.e., noble gases (He, Ne, Ar, Kr, Xe), Schottky defects, and the interaction between these defects. We found the following: (1) collinear antiferromagnetic UO_2 has an energy-lowering distortion of the oxygen sublattice from ideal fluorite positions; (2) DFT + U qualitatively affects the formation volume of Schottky defect clusters in UO_2 (without U the formation volume is negative, but including U the formation volume is positive); (3) the configuration of the Schottky defect cluster is dictated by a competition between electrostatic and surface energy effects; (4) the incorporation energy of inserting noble gas atoms into an interstitial site has a strong dependence on the volume of the noble gas atom, corresponding to the strain it causes in the interstitial site, from He (0.98 eV) to Xe (9.73 eV); (5) the energetics of each of the noble gas atoms incorporated in Schottky defects show strong favorable binding, due to strain relief associated with moving the noble gas atom from the highly strained interstitial position into the vacant space of the Schottky defect; and (6) for argon, krypton, and xenon, the binding energy of a noble gas impurity with the Schottky defect is larger than the formation energy of a Schottky defect, thereby making the formation of Schottky defects thermodynamically favorable in the presence of these large impurities.

DOI: 10.1103/PhysRevB.84.134111 PACS number(s): 71.15.Mb, 61.72.J−, 24.75.+i

I. INTRODUCTION

In uranium dioxide, a nuclear fuel, energy is produced by a fission reaction where uranium is transmuted into another element. Xenon is one element produced in the fission reaction of uranium, and xenon atoms tend to coalesce into bubbles in uranium dioxide. Xenon bubbles cause the fuel pellet to swell and can adversely affect the fuel properties. The atomistic mechanisms underlying the swelling, such as the nucleation and growth of the xenon bubbles, are not well understood. For instance, the size and shape of critical nuclei of xenon bubbles are unknown. To help develop such an understanding, we would need to know the energetics of defects associated with the xenon bubble nucleation. Density functional theory (DFT) is a method that has proved reliable in studying point defect energies in atomic-scale calculations.[1–5] There are many previous calculations of the properties of pure, bulk UO_2 from both DFT[6–14] and classical potentials.[7,8,15–19] However, a DFT study of *defects* in UO_2 is complicated by the magnetic and electronic structure of this material.

The complex magnetic structure of UO_2 leads to difficulties in achieving an accurate description from DFT. UO_2 is an insulating paramagnet in the fluorite (CaF_2) structure at room temperature.[20] At low temperatures, UO_2 is an antiferromagnet, with a Néel temperature of 30.8K. The orientation of magnetic moments in UO_2 has been the subject of some discussion in the literature.[20–22] Comparing calculated and measured electric field gradients, Laskowski *et al.*[21] and Ikushima *et al.*[22] found that the low-temperature magnetic structure of UO_2 is noncollinear. The noncollinear antiferromagnetic (AFM) structure is shown in Fig. 1, along with a simpler, collinear arrangement. The noncollinear magnetic moments lie in [111]-type directions, with a corresponding distortion of the oxygen sublattice also in [111]-type directions. However, uranium dioxide is of interest as a nuclear fuel at high temperatures when it exhibits a paramagnetic structure. Paramagnetic structures are not easily simulated with DFT, due to the lack of long-range periodic order of the magnetic moments. Paramagnetic dynamical mean field theory (DFT) calculations have recently been performed on UO_2.[23] The paramagnetic phase, which has no net magnetic moment, could be approximated by a nonmagnetic calculation, but as we show later, this severe approximation leads to a metallic ground state in DFT. A true paramagnetic state has a disordered distribution of nonzero magnetic moments. A nonmagnetic calculation does not capture these local magnetic moments. Another approximation to the paramagnetic state that does include local magnetic moments (albeit in a long-range-ordered arrangement that lends itself to standard DFT calculations) is an AFM ordering.

Another complication when performing DFT calculations of UO_2 lies in the complex electronic structure of this compound. UO_2 is a Mott-Hubbard insulator:[24] in DFT, Mott-Hubbard insulators are incorrectly found to be metallic in standard DFT due to the poor description of electron–electron correlations.[25] Methods that go beyond standard DFT exchange correlations can yield a band gap in UO_2, like self-interaction corrected local density functional theory (SIC-LDA)[26] and hybrid functionals.[27,28] The density functional theory + U (DFT + U) method (often referred to as LDA + U) can also correct this deficiency and yield an insulating solution in UO_2. Dudarev *et al.* calculated UO_2 within the DFT + U method and found a 1.1-eV band gap.[24] Thus, the use of DFT + U methods qualitatively alters the electronic structure of UO_2 and hence may alter other properties, such as defect energetics of noble gases in UO_2. Despite the successes of DFT + U in describing UO_2, another difficulty of this method lies in the possibility of converging to multiple self-consistent solutions (with different total energies) corresponding to different electron orbital occupations.[6,24,29] Recently, Meredig *et al.* proposed an efficient "U-ramping" method to find a low-energy self-consistent solution within a DFT + U approach.[29]

Despite these difficulties, there are many examples in the literature of the application of DFT-based methods to noble

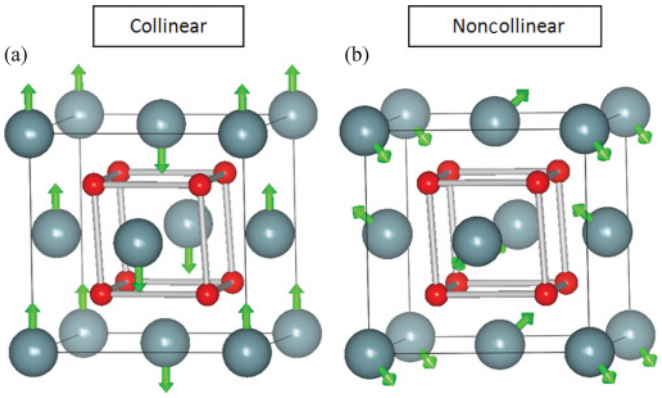

FIG. 1. (Color online) The AFM structure of UO_2 in the (a) collinear and (b) noncollinear geometries. The large (gray) atoms are uranium, and the small (red) atoms are oxygen. The (green) arrows indicate the direction of the magnetic moment on the uranium atoms. The oxygen atoms are shown with a "cage" to draw attention to the distortion in the oxygen sublattice. We find that DFT + U predicts an energy-lowering oxygen distortion in the collinear geometry, similar to the distortion known to occur in the [111]-type directions seen in the noncollinear ground state.

gas impurities in UO_2. However, these previous studies yield significantly disparate results. Freyss *et al.*[10] calculated helium and xenon interstitials in nonmagnetic UO_2 with DFT (no U) and found xenon incorporation to be very unfavorable (11.2 eV) but somewhat surprisingly found that helium incorporation to be slightly favorable (-0.1 eV). Petit[11] calculated the incorporation energies of helium and krypton in various sites (interstitials, vacancies, Schottky defect, or SD, clusters, etc.) in nonmagnetic UO_2 with DFT (no U) and found that the energy to incorporate the noble gas atom into SDs is much less than that needed to incorporate them into interstitials. Yun *et al.*[12,13] used DFT (no U) and an AFM state to calculate helium and xenon in interstitial sites and various cavities in UO_2 and surprisingly found the incorporation energy of xenon into an interstitial was less than the incorporation energy of helium into an interstitial, even though xenon is a significantly larger atom. This result differs from the calculation of Freyss *et al.* by more than 11 eV. Yun *et al.*[14] also performed nudged elastic band calculations on potential diffusion pathways for xenon in UO_2. These previous studies often included significant approximations for the magnetic and electronic structure of UO_2. In all of the previously mentioned studies, the calculations were performed without the DFT + U methodology, leading to a qualitatively incorrect (metallic) electronic structure for UO_2. Since the electronic structure affects the defect energies in UO_2, the use of DFT + U may be necessary for quantitatively accurate defect energies.

More recent studies of UO_2 have used DFT + U. Gryaznov *et al.*,[30] calculated helium in UO_2, and, like Freyss *et al.*,[10] found a negative incorporation of helium into the interstitial position of UO_2. Geng *et al.*[31] and Nerikar *et al.*[32] separately calculated the incorporation energy of xenon in an interstitial and found the defect energies differ by > 1 eV (9.75 eV for the former and 11.11 eV for the latter). This spread in defect energies could indicate that at least one of these calculations has converged to a metastable orbital occupation for the defect calculation, the reference state of pure UO_2, or both.

Given the wide disparity in previous result and methods, we assert that an extensive, systematic series of defect calculations in UO_2 is needed. We calculated a series of noble gas impurities in UO_2 from helium to xenon to find the trends of the energetics of increasing the defect size. We accurately modeled UO_2 as an insulator with DFT + U, rather than the qualitatively incorrect, metallic solution given by conventional DFT (no U). Our calculations have shown that even the collinear AFM state of UO_2 has an energy-lowering distortion of the oxygen sublattice. In addition, we found an unexpected consequence of DFT + U on SD cluster geometries: upon removing a single UO_2 unit from the lattice, DFT (no U) gives a contraction of the lattice, whereas DFT + U gives an expansion of the lattice. We also found that noble gas atoms cause large amounts of strain energy in interstitial sites and much of that strain can be relieved by placing the noble gas atom into a SD cluster. For the large noble gas atoms (argon, krypton, and xenon), the strain energy for interstitial insertion is so large that the system could actually lower its energy by the formation of a SD (with noble gas atom inside).

II. METHODOLOGY

We performed electronic structure calculations using spin-polarized DFT via the Vienna *ab initio* simulation package (VASP).[33–36] We used the Perdew-Wang '91[37] (PW91) generalized gradient approximation (GGA) with the effective + U (U = 3.99 eV) correction for strongly correlated systems as described by Dudarev *et al.*[38] Our energy cutoff was 500 eV with a $2 \times 2 \times 2$ gamma-centered k-point grid for 96-atom calculations and $4 \times 4 \times 4$ grid for 12-atom calculations. We compared our total energies with those from a Monkhorst-Pack k-point grid and found no appreciable difference from the gamma-centered grid. We used a 12-atom cell for collinear and noncollinear calculations of pure UO_2 without defects. We used a 96-atom UO_2 supercell with collinear AFM ordering for defect calculations. The initial magnitude of the magnetic moment was 2 μB for collinear calculations and 2 μB in the x, y, and z directions for noncollinear calculations. We also used the Vosko, Wilk, and Nusair interpolation of the magnetic states.[39] All degrees of freedom (cell shape, volume, and internal coordinates) were relaxed consistent with the initial symmetry of the cell. In some cases noted later, we even considered symmetry-lowering relaxations. During relaxations, forces were minimized to a threshold value <20 meV/Å.

DFT + U calculations can converge to different self-consistent energy solutions for UO_2.[29,40] These multiple solutions represent possible orbital occupancies. The existence of these different self-consistent solutions can make it difficult to find the true ground state energy and hence might have a significant effect on defect energetics. We found that the lowered symmetry of our cell due to the distortion in the oxygen sublattice makes it more likely for the self-consistency process to converge to the true ground state (or at least a low-energy occupation). We confirmed our orbital occupations for pure UO_2 corresponded to low-energy orbital occupations by using a recently proposed U-ramping method[29] for finding low-energy orbital occupations by guiding the calculation

though increasing U values. In Ref. 29, it was demonstrated that for low-symmetry calculations, the spread in energy of the different orbital occupations is reduced and the lowest-energy state is more easily found (i.e., reduction in symmetry reduces the likelihood of getting trapped in high-energy metastable states). We observed that the lowered symmetry of our UO_2 with oxygen distortions, similar to the conclusions of Ref. 29, seems to reduce the spread in energy of the different orbital occupations. Direct use of the method of Ref. 29 for our series of defect calculations would be computationally prohibitive. Hence, for the majority of the calculations shown here, we used a different scheme as follows: We applied the U-ramping method described in Ref. 29 to calculations of pure UO_2 (without any defects and with oxygen atoms moved slightly from high-symmetry positions) to find the ground state occupations at the final value of U = 3.99 eV. The defect calculations were performed with the final value of U = 3.99 eV, and starting at the pure, distorted UO_2 geometry, a full atomic relaxation was performed at this high-U value. To test this approach, we compared this modified method with the U-ramping method for SD calculations. The U-ramping procedure was slightly modified to accommodate the defect calculations for these test cases. Starting from the geometry of the relaxed defect cell (calculated with the initial change density and wave functions from bulk UO_2), we slowly ramped the U value for those calculations by increments of 0.1 eV from U = 0.0 eV until U = 1.0 eV and then jump to U = 3.99 eV at fixed geometry. After self-consistent convergence at the final U value, we subsequently fully relaxed all degrees of freedom. This modification of the U-ramping procedure was made for computational efficiency.

For the three SD energies (SD1, SD2, and SD3, defined below), we performed tests using our modified U-ramping method (Ref. 29) to determine whether the issue of metastable electronic minima was significantly affecting our defect energies. The comparison between the U-ramping and the simpler method of starting from the bulk orbital occupations gives nearly degenerate results. The modified U-ramping method actually gives slightly higher energies, by 0.27–0.96 meV/atom (25–89 meV/SD). This difference in energy is relatively small, compared to the energy scale of the defects considered in this work. We found lower-energy orbital occupations by starting from the defect-free ground state geometry, rather than by using the U-ramping method, which is somewhat surprising. Ramping more slowly through U values might help converge to the lower-energy states, but it would also increase the computational cost. For SD1, we performed the U-ramping method with a smaller step size (0.05 eV) near the critical U point (0.1–0.4 eV). With the smaller step size, the discrepancy was reduced from 0.30 to − 0.05 meV/atom (29 to − 4 meV/SD). The results of all these tests give us confidence that our defect energies are not significantly affected by the problem of multiple electronic minima, perhaps due to the lowered symmetry of the simulation cell caused by the oxygen distortion.

III. RESULTS

A. Structure and properties of pure UO_2

As mentioned previously, there are difficulties associated with an accurate DFT calculation of the electronic and magnetic state of UO_2. Because of these difficulties, we first explore the effects of using different levels of theory and magnetic ordering on the properties of UO_2. Table I gives results from our calculations of UO_2, along with several other DFT calculations of UO_2 in the literature. Across

TABLE I. Comparison of bulk modulus, volume, and magnetic moment of bulk UO_2 calculated from DFT and DFT + U. The first four calculations are from the present study, and the other calculations are from previous studies. The band gap for the present GGA + U calculation is higher than other reported values due to the oxygen distortion. Dorado *et al.* (Ref. 43) also calculated this distortion but did not report a band gap. FM, ferromagnetic; NM, nonmagnetic.

			B (GPa)	Volume/unit cell (Å^3)	Magnetic moment (μB)	Gap (eV)	U-J	Method	Ref.
	GGA	FM	198	155	1.98	0		VASP	
Present	GGA	AFM	188	158	1.40	0		VASP	
Work	GGA	NM	205	159	0	0		VASP	
	GGA + U	AFM	188	170.5	2.01	2.8	3.99	VASP[a]	
	LDA	AFM	239.99	151		0		VASP	31
	GGA	Not specified	203.53	160		0		VASP	31
	LDA + U	AFM	208.3	161	1.93	1.45	4	VASP	31
Previous	GGA + U	AFM	180.68	171	1.93	1.6	4	VASP	31
Studies	GGA	NM	209	156	0	0		VASP	44
	GGA	AFM	188	157	1.44	0		VASP	44
	GGA + U	AFM	209	168	1.94	1.8	4	VASP	44
	GGA	NM	195	158	0	0		ABINIT	10
	GGA + U	AFM					3.3		45
	GGA + U	AFM	187	170.3		2.3	3.99	ABINIT	40
	Hybrid	AFM	199	167	1.75	1.98		ABINIT	40
	LDA + U	AFM	202	163	1.7	2.1	4		46
	Exp.	AFM	207	164	1.74	1.8		Exp.[a]	44

[a]Distortion in oxygen sublattice.

several combinations of DFT + U and magnetism, calculated properties such as lattice parameter and bulk modulus are within the expected error of DFT. But previous calculations found that DFT (no U) produces a metallic solution for UO_2 rather than an insulating one.[24] Our calculations confirm this finding. In some previous studies, it was assumed that because the structural properties are close to the experimental values, the nature of the metallic versus insulating state may not be important to achieving accurate energetic properties.[13] Because the existence of an insulating versus metallic solution involves a qualitative change in the electronic structure, which is intimately tied to the total energy, we use DFT + U to obtain the correct insulating behavior in our electronic structure calculations. We later examine the effect of DFT with and without U on defect energies and geometries.

The calculations in Table I using DFT + U show increased volumes compared to calculations only using DFT (no U). The bulk moduli among the different magnetic states are consistent for GGA (no U) but vary for GGA + U (a 15% difference between the highest and the lowest values). This variation may be due to the presence of different self-consistent solutions present in the different researchers' DFT + U calculations. While there were several bulk modulus values reported for GGA + U, the volume of UO_2 was more consistent among the calculations (a 1.8% difference between the largest and the smallest volumes). Dorado *et al.*[40] performed an extensive examination of the possible orbital occupations in UO_2 (without oxygen distortions) that occur with DFT + U. While there are some differences our calculation method and those of Ref. 40 (Dorado *et al.* use Lichtenstein for DFT + U), we find good agreement with the bulk modulus and equilibrium volume of Dorado *et al.*[40]

While some bulk properties of UO_2 are similar for DFT (metallic) and DFT + U (insulating), the different electronic states have different magnetic ground states. A comparison of the relative energies for different magnetic states, with and without the + U parameter, is shown in Table II. The lowest-energy solution for DFT (no U) is metallic, ferromagnetic UO_2. Some previous studies of defects in UO_2 perform DFT (no U) and use a collinear AFM state[12–14,41,42] rather than the lower-energy ferromagnetic state. The lowest-energy solution for DFT + U is insulating, collinear AFM UO_2 with a distortion in the oxygen sublattice. The oxygen distortion is discussed in more detail later. This distortion lowers the energy of collinear AFM UO_2 below that of noncollinear AFM UO_2, where the latter is the low-temperature experimentally observed state.[20] Thus, standard DFT + U does not predict the observed ground state of UO_2 as the lowest-energy structure. The resolution of this apparent discrepancy was recently found by Zhou and Ozolins,[6] who used a self-consistent DFT + U approach with a model Hamiltonian to treat self-interaction errors and found that the observed noncollinear 3k was the lowest-energy state in their calculations, though the collinear AFM state is close in energy. Since the collinear AFM state has the lowest energy for standard DFT + U calculations and is computationally less expensive than the noncollinear state, we use the collinear magnetic state in our defect calculations.

B. Oxygen positions

Below the Néel temperature, experiments show the oxygen ions are distorted from the ideal fluorite sites in [111] directions.[20] This distortion has been verified with DFT + U calculations that included noncollinear magnetism.[21,47] Some previous DFT studies[21,22] of UO_2 with collinear magnetism did not report any oxygen sublattice distortion, but we find that a symmetry-lowering distortion of the oxygen ions lowers the energy even for a collinear magnetic geometry. A distortion in the oxygen sublattice was reported by Gryaznov *et al.*,[30] as well as by Dorado *et al.* for collinear AFM.[43] This distortion does not occur upon standard atomic relaxation when beginning from the fluorite positions because the distortion is not symmetry preserving. To find the distortion in our collinear DFT + U calculations, we first manually distort the oxygen positions with [111]-type distortions, and then we follow this with a geometry relaxation. The oxygen atoms do not relax back to the fluorite positions; rather, they undergo an energy-lowering distortion in the [2.66 1.95 1]-type directions instead of the distortions in the [111]-type directions that occur in the noncollinear case (in DFT + U and experimentally). The energy of the distorted UO_2 structure is lowered by 77 meV per formula unit (f.u.) compared to the fluorite positions. The magnitude of the displacement is 0.09 Å. The size of displacement in our noncollinear

TABLE II. DFT and DFT + U calculations of nonmagnetic, ferromagnetic, and AFM states of UO_2. The lowest-energy magnetic structure for DFT (no U) is ferromagnetic UO_2. The lowest-energy magnetic structure for DFT + U is collinear AFM UO_2 with an energy-lowering distortion of the oxygen sublattice. FM, ferromagnetic; NM, nonmagnetic; OD, oxygen distortion.

Method	Magnetic structure	Relative energy (eV/f.u.)	Magnetic moment (μB)	Conductivity
DFT (no U)	NM	0.202	0	Metallic
	FM	0.000	1.98	Metallic
	Collinear AFM	0.158	1.40	Metallic
	Noncollinear AFM	0.175	1.36	Metallic
DFT + U	NM	2.177	0	Metallic
	FM	0.163	2.02	Insulating
	Collinear AFM	0.077	1.52	Insulating
	Collinear AFM (OD)	0.000	2.01	Insulating
	Noncollinear AFM	0.058	1.97	Insulating

AFM calculations is 0.016 Å. Zhou and Ozolins[47] found the displacement to be 0.024 Å in their noncollinear AFM calculations. Dorado *et al*. found the distortion to be 0.16 Å in the case of collinear AFM and 0.009 Å in the case of noncollinear AFM.[43] Measurements from neutron diffraction found the displacement to be 0.014 Å.[20] It is not clear why the oxygen distortion calculated with collinear AFM were larger than the noncollinear AFM oxygen distortion, but it is important to include this distortion in defect calculations. When a defect is added, the high symmetry of ideal fluorite (which prevents the oxygen atoms from distorting in bulk, defect-free, symmetry-preserving calculations) is lowered by the presence of the defect and the oxygen atoms undergo the distortion, even in symmetry-preserving defect calculations. If UO_2 is used as a reference energy for the defect energies, restricting the oxygen to fluorite positions in defect-free UO_2 but allowing them to distort around the defect causes significant errors in defect energies. For our defect calculations described later, we use the reference state of UO_2 as the collinear AFM magnetic state with the oxygen distortions and DFT + U (U = 3.99), as this represents the lowest-energy magnetic structure.

C. Defect energetics

After UO_2 undergoes fission, many defects are incorporated into the material, such as vacancy clusters and impurity atoms. We do not expect noble gas atoms to chemically interact significantly with UO_2. However, noble gas atoms cause strain in the lattice, the amount of which is a function of noble gas size. In the limit of dilute additions, the strain energy increases linearly with the number of noble gas atoms. The strain could be relieved if a cavity was created to nucleate a bubble, but a cavity has an energetic penalty in the form of surface energy. The tradeoff between this strain energy reduction and the surface energy penalty controls the stability of gas-filled bubbles. As the bubble size and number of gas atoms grow larger, the strain relief of noble gas atoms in bubbles eventually becomes larger than the surface energy of the bubble (which scales as the surface area of the bubble), causing the bubble of that size to become energetically favorable. The schematic in Fig. 2 shows two scenarios for multiple noble gas atoms in UO_2: (a) the noble gas atoms are in interstitial positions, causing large amounts of strain energy, and (b) the noble gas atoms are in a cavity, forming a small bubble that relieves strain by giving the large xenon atoms extra space, but at the cost of the surface energy needed to create the cavity. We show later how our DFT calculations of interstitial gas impurities and SDs can be used to estimate this tradeoff between strain and surface energies, and we determine the number of gas atoms for which the strain energy from the dispersed noble gas atoms becomes larger than the energy penalty of creating a cavity for the noble gas atoms.

Here, we use DFT + U to calculate these defect energies in UO_2. We consider SD clusters (two oxygen vacancies and one uranium vacancy), noble gas impurities, and combinations of SDs and noble gas atoms. We have performed DFT + U calculations of various defects within a 96-atom UO_2 supercell, including collinear AFM order and oxygen distortions from ideal fluorite positions: (1) interstitial noble gas atoms (He, Ne, Ar, Kr, and Xe), (2) SD clusters (trivacancies), and (3) noble gas atom–Schottky defect (NG-SD) complexes. We used the series of five noble gas atoms to gauge the effect of increasing atom size on the defect energetics.

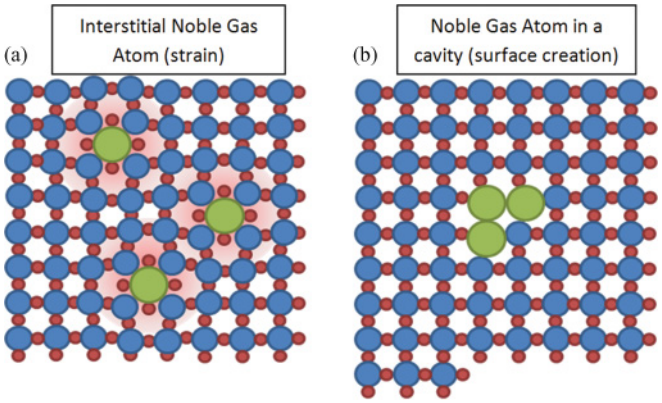

FIG. 2. (Color online) (a) Noble gas atoms in the interstitial sites of UO_2 induce strain, indicated by pink areas. (b) The strain can be relieved by creating a cavity for a bubble to form. There will be a point at which the savings of relieving the strain energy of the dispersed noble gas atoms outweigh the cost of creating the bubble to contain those atoms.

Next, we define several types of defect energies we have calculated for noble gas atoms in interstitials, SD clusters, and NG-SD complexes. We next illustrate these defect energies for the case of xenon impurities, but analogous equations exist for other noble gas impurities.

Xenon incorporation energy ($\Delta E^{\text{Inc.}}_{\text{Xe}}$): This quantity is the energy of incorporating a xenon atom into the octahedral interstitial site of UO_2 relative to pure UO_2 and an isolated xenon atom,

$$\Delta E^{\text{Inc.}}_{\text{Xe}} = E(N \cdot \text{UO}_2 + \text{Xe}_i) - N \cdot E(\text{UO}_2) - E(\text{Xe}), \quad (1)$$

where $E(N \cdot \text{UO}_2 + \text{Xe}_i)$ is the energy of xenon in the interstitial position of a supercell with N UO_2 formula units. $E(\text{UO}_2)$ is the energy per formula unit of bulk UO_2. As stated previously, the reference energy of UO_2 in all cases corresponds to the geometry with low-energy oxygen distortions. $E(\text{Xe})$ is the energy of a single, isolated xenon atom.

SD formation energy (ΔE^{f}_{SD}): The SD formation energy is just the energy cost associated with creating the trivacancy defect in UO_2,

$$\Delta E^{f}_{\text{SD}} = E((N-1) \cdot \text{UO}_2) - (N-1) \cdot E(\text{UO}_2), \quad (2)$$

where $E((N-1) \cdot \text{UO}_2)$ is the energy of supercell with N UO_2 formula units minus one UO_2 formula unit (the SD). We discuss the specific geometry of the trivacancy SD later.

SD–xenon atom solution energy ($E^{\text{Sol.}}_{\text{Xe–SD}}$): This solution energy is the energy of a SD cluster with xenon inside relative to perfect UO_2 and an isolated xenon atom,

$$\Delta E^{\text{Sol.}}_{\text{Xe–SD}} = E((N-1) \cdot \text{UO}_2 + \text{Xe}) - (N-1) \cdot E(\text{UO}_2) - E(\text{Xe}), \quad (3)$$

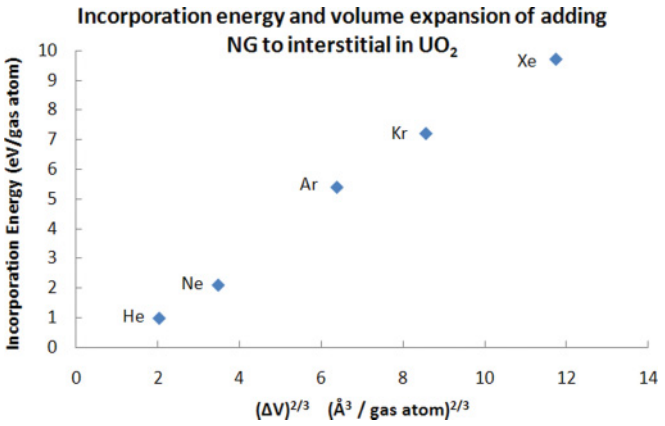

FIG. 3. (Color online) DFT + U calculations of the incorporation energy of noble gas atoms into interstitial positions of UO_2 [Eq. (1)] versus the difference in volume of the simulation cell with and without the noble gas atom (ΔV) to the two-third power. The change in volume scales with $(\Delta a)^3$, and the strain scales as $(\Delta a)^2$. As the size of the noble gas atom increases, the incorporation energy increases.

where $E((N-1)\cdot UO_2 + Xe)$ is the is the energy of supercell with N UO_2 formula units minus one UO_2 formula unit (the SD) plus a xenon atom.

Xenon incorporation energy into preexisting SD clusters: This incorporation energy is the energy of a SD cluster with xenon inside relative to an "empty" SD cluster and an isolated xenon atom,

$$\Delta E^{\text{Inc.}}_{\text{Xe-SD}} = E((N-1)\cdot UO_2 + Xe) - E((N-1)\cdot UO_2) - E(\text{Xe atom}) = \Delta E^{\text{Sol.}}_{\text{Xe-SD}} - \Delta E^{f}_{\text{SD}}, \quad (4)$$

where instead of referencing $N-1$ formula units of pure UO_2, the defect is referenced to a SD, $E((N-1)\cdot UO_2)$.

Binding energies of NG-SD complexes: The binding energy is the difference between the xenon atom in a SD and the two defects at infinite separation (xenon atom in an interstitial and an empty SD cluster):

$$E_{\text{Bind}} = \Delta E^{\text{Inc.}}_{\text{Xe}} + \Delta E^{f}_{\text{SD}} - \Delta E^{\text{Inc.}}_{\text{Xe-SD}}. \quad (5)$$

Analogous equations to Eqs. (1)–(5) apply for other noble gas atoms considered here (He, Ne, Ar, and Kr).

1. Noble gas atom incorporation energies

Figure 3 shows DFT + U incorporation energies [Eq. (1)] of noble gas atoms into interstitial sites as a function of the volume increase of the simulation cell due to adding the noble gas atom. Although all values of $\Delta E^{\text{Inc.}}$ are large and positive, we find that the incorporation energy has a strong dependence on the size of the atom. The larger the noble gas atom, the larger the energy needed to incorporate it into the lattice. For instance, it takes 9.73 eV to incorporate the large xenon atom into an interstitial site but only 0.98 eV to incorporate the much smaller helium atom. We expect that the dominating contribution to this defect energy is strain. In principle, there could be van der Waals interaction, but we expect this nonbonded interaction to be much smaller than the strain energy.

2. SD cluster energetics

For the SD clusters, we removed one uranium atom and two neighboring oxygen atoms from the lattice. In the perfect CaF_2 lattice, there are only three configurations for the constituent vacancies for this defect, assuming each oxygen vacancy must be a nearest neighbor of the uranium vacancy. These three SD clusters differ by how close the two oxygen vacancies are to one another, the possibilities being first- (SD1), second- (SD2), and third- (SD3) nearest-neighbor oxygen vacancies. In principle, not all SD configurations of the same type are symmetrically equivalent due to oxygen sublattice distortions and distortions in the unit cell shape, leading to energetic differences ($\leqslant$0.120 eV for SD1), but the differences are small compared to noble gas incorporation energies. The three configurations of SD clusters differ in energy by 0.76 eV. Our calculated SD energies can be explained by a combination of electrostatic and surface energy considerations. From purely electrostatic considerations, the distance between the oxygen vacancies and the uranium vacancy should be minimized to maximize the coulombic attraction between them, while the distance between the two oxygen vacancies should be maximized to minimize the coulombic repulsion between them. This set of requirements yields a linear complex with oxygen vacancies at the ends and the uranium vacancy in the center. In UO_2, this configuration has the oxygen vacancies as third-nearest neighbors. However, the surface energy contribution would favor vacancies clustered as close as possible to one another to reduce the number of unsatisfied bonds. In UO_2, the most compact SD cluster has the oxygen vacancies as nearest neighbors. Thus, electrostatics favors the SD3 geometry and surface energies favor the compact SD1 geometry. In our calculations, neither the low surface energy configuration ($\Delta E^{f}_{\text{SD1}} = 4.09$ eV) nor the low electrostatic energy configuration ($\Delta E^{f}_{\text{SD3}} = 3.45$ eV) is the lowest-energy configuration in UO_2; rather, the configuration with oxygen vacancies as second-nearest neighbors ($\Delta E^{f}_{\text{SD2}} = 3.33$ eV) is the energetically preferred vacancy cluster. The configuration of the vacancies is energetically a balance between surface energy and electrostatics.

3. SD cluster geometry and formation volume

We next compute the relative formation volume of the SD cluster (ΔV^f), i.e., the volume added or removed to the material due to the addition of the SD,

$$\Delta V^f = V_{(N-1)\cdot UO_2} - V_{N\cdot UO_2}, \quad (6)$$

where $V_{(N-1)\cdot UO_2}$ is the volume of the cell with a N formula units of UO_2 minus a single formula unit (a SD cluster) and $V_{N\cdot UO_2}$ is the volume of the perfect UO_2 cell with N formula units (V_{SD} has one less UO_2 unit than V_{perfect}). For $\Delta V^f > 0$, removing the atoms associated with the SD causes an expansion of the lattice, and for $\Delta V^f < 0$, a contraction of the lattice. Interestingly, the relative formation volume of the SD cluster (SD1) was positive for AFM calculations with DFT + U ($\Delta V^f = 5.93$ Å^3). When DFT + U was not used, the relative formation volume was negative ($\Delta V^f = -1.95$ Å^3). With DFT + U, the larger volume for the SD leads to a decrease in the strain of noble gas atoms inside SDs compared to the

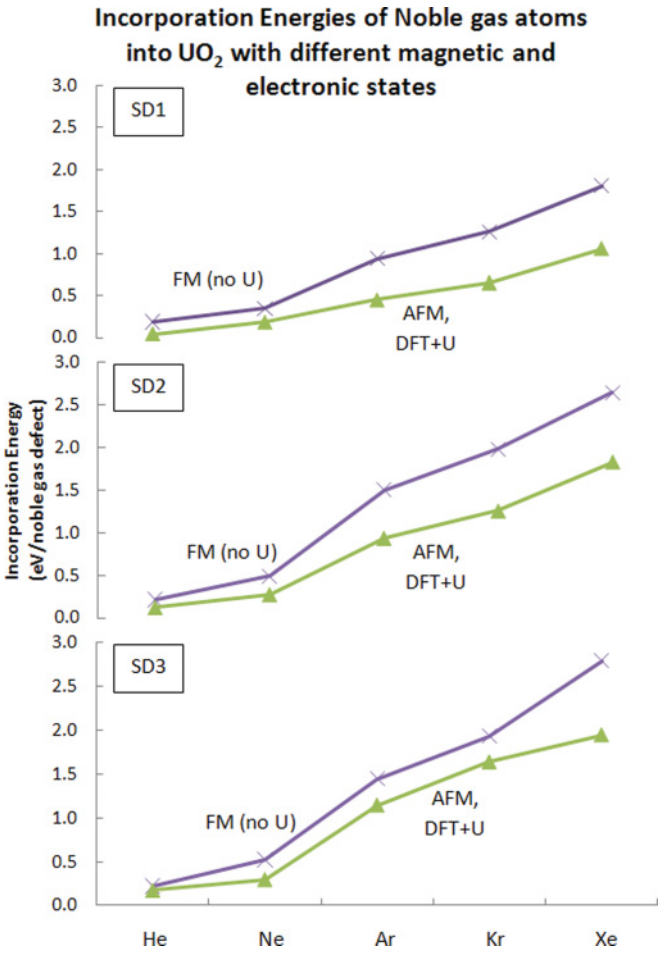

FIG. 4. (Color online) Incorporation energies of noble gas atoms into preexisting SDs in UO_2 [Eq. (4)]. We show results for all three SD geometries (SD1, SD2, and SD3) using both DFT + U (AFM, insulating) and DFT (no U) (ferromagnetic, metallic). AFM DFT (no U) UO_2 shows similar behavior to ferromagnetic UO_2. SDs formed in insulating, AFM UO_2 are larger than SDs formed in metallic (anti- or ferromagnetic) UO_2, thereby allowing more space for noble gas atoms to reside and decreasing the associated strain. Because the metallic calculations have smaller SDs, the noble gas atoms are in a tighter space, causing more strain and larger incorporation energy.

smaller volume of DFT (no U). The smaller strain energy in DFT + U decreases the incorporation energy of noble gas atoms into the SD compared to DFT (no U). Figure 4 shows incorporation energy of noble gas atoms into the three SDs [Eq. (3)] with DFT (no U) and with DFT + U. The energetics of NG-SD complexes are discussed in more detail later.

Many examples demonstrate that the relative formation volume of vacancies in metallic systems is negative (e.g., see Refs. 48–50) but can be positive for ionic solids such as δ-Bi_2O_3.[51] A recent review of 19 UO_2 pair potentials showed that all but 2 give a positive formation volume of the SD.[17] We examined this positive formation volume further by creating a simplified electrostatic point charge model of UO_2 in the fluorite structure with formal charges of − 2 for O and + 4 for U. We calculated the forces on the atoms in this point charge model and observed that the atoms neighboring the SD cluster have a force pointing away from the SD cluster. In an ionic system, an ion is surrounded by ions of opposite charge, attracting them. When a UO_2 unit is removed from the lattice, the attractive force each ion produced is also removed, leaving the like-charged neighbor ions to repel each other. The removal of the attractive force acts like a repulsion, giving a positive relative formation volume. Without GGA + U and magnetism, the system is not ionic but metallic, leading to a formation volume of the SD cluster that is qualitatively incorrect. This volume difference could affect previous calculations[10,41] of noble gas impurities calculated with DFT (no U). To ensure that the positive Schottky formation volume is not simply an erroneous artifact of DFT + U, we also performed DFT (no U) calculations for a simple ionic system where DFT + U is not required to obtain an insulating solution, i.e., CaF_2 in the fluorite structure. DFT calculations of a SD in CaF_2 showed the same positive relative formation volume for a SD cluster.

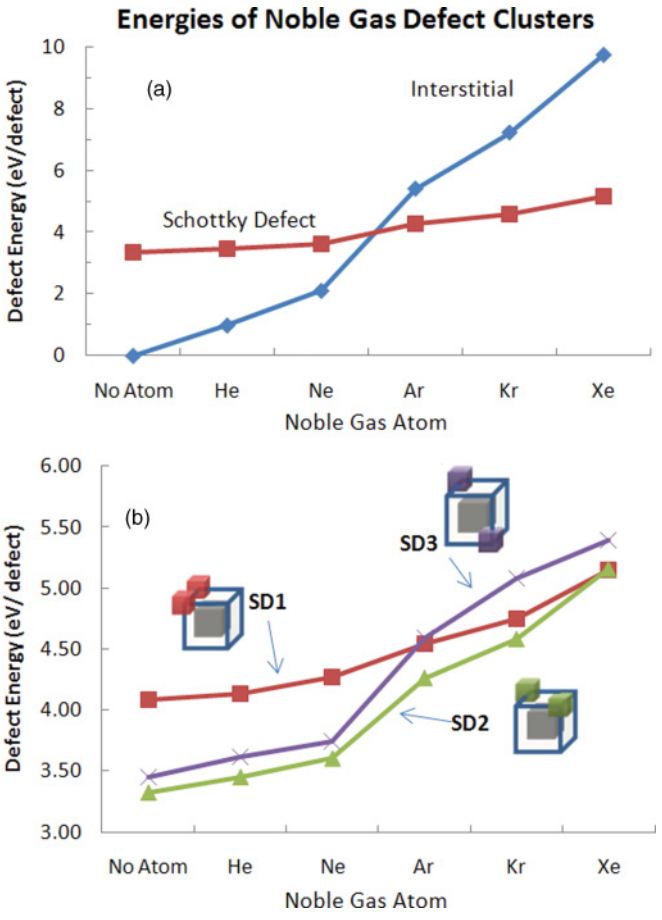

FIG. 5. (Color online) DFT + U calculated incorporation energies of interstitial noble gas atoms [Eq. (1)], formation energy of SD clusters [Eq. (2)], and solution energy of NG-SD complex defect complexes [Eq. (3)]. (a) The interstitial noble gas energies and energies of NG-SD complexes (lowest-energy configuration for each noble gas atom shown). (b) The energies of all SD configurations of NG-SD complex. The SD cluster geometries (SD1, SD2, and SD3) are illustrated (the large cube is a uranium vacancy, and the smaller cubes represent oxygen vacancies; the wireframe cube represents the cubic sublattice of oxygen in the fluorite structure). Tabulated values are given in Table III.

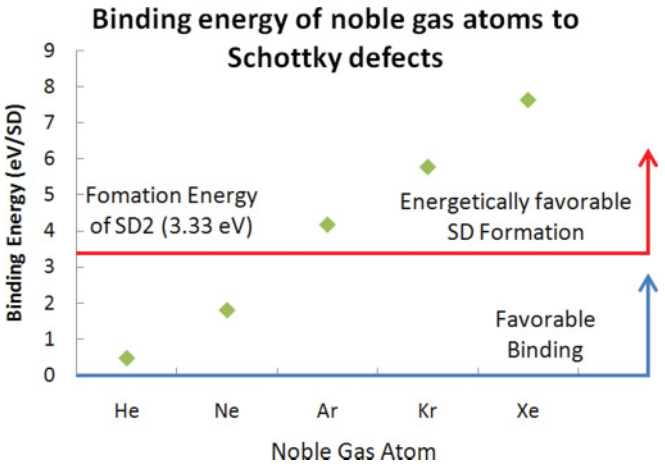

FIG. 6. (Color online) DFT + U binding energies of noble gas atoms to SD clusters [Eq. (5)]. All noble gas atoms favorably bind to the SD. Argon, krypton, and xenon have binding energies larger than the formation energy of a SD (3.33 eV), meaning it is energetically favorable to form a Schottky defect and place the noble gas atom in it.

4. Noble gas atom: SD complex

We calculate solution energies [Eq. (3)] for each of the noble gas atoms (He-Xe) inside the cavity formed by each of the three SD cluster configurations (SD1, SD2, and SD3). We compare the formation energies of the various geometries and the incorporation energy of noble gas atoms into the interstitial sites (Fig. 5). Just as for the case of a noble gas interstitial, the energy of the NG-SD complex is dominated by strain. The energy increases as the size of the noble gas increases, but not as dramatically as when the noble gas atoms were in the smaller interstitial sites. Adding a helium atom into the SD only slightly increases the solution energy of the defect cluster over the formation energy of the vacant SD (∼0.04 eV). Increasing the size of the noble gas atom also changes the energetic preference of the SD configurations. For example, the vacant second-nearest-neighbor oxygen vacancy configuration (SD2) was 0.76 eV lower than in the SD1 configuration, but when xenon is added, the more compact SD1 is slightly preferred to SD2.

At the beginning of Sec. III C, we discussed the stability of placing noble gas atoms separately in interstitial positions versus collectively in a bubble. We argued that there would be a specific size of the bubble (or number of noble gas atoms) beyond which the noble gas atoms would energetically prefer a bubble rather than interstitial positions (see Fig. 2). From our calculations described previously, we now see that for the large noble gas atoms (argon, krypton, and xenon), *the NG-SD complex is energetically preferred over a single noble gas atom in an interstitial site*. Placing these very large atoms in an interstitial causes so much strain that it would be energetically favorable to form a SD cluster and place the noble gas atom in it to partially relieve the strain. (For the formation of the SD, we assume the system to be in equilibrium with a bulk reservoir of UO_2 and the atoms removed to create the SD become part of the reservoir.) For these large atoms, the energetic gain of strain relief overwhelms the energetic cost of creating the SD. Xenon is such a large atom that placing it in the interstitial site has more than double the defect energy of creating a xenon–SD cluster. Thus, having these large noble gas atoms in interstitial site is a highly unfavorable thermodynamic situation. All noble gas atoms are bound to the SD (all configurations), and Fig. 6 shows the binding energy of noble gas atoms to SD2.

IV. COMPARISON OF PRESENT RESULTS AND PREVIOUS DFT AND CLASSICAL POTENTIAL ENERGIES

Noble gas atoms in UO_2 have been the subject of many previous computational studies. Table IV gives incorporation energies of noble gas atoms into interstitial sites in UO_2 [Eq. (1)] from previous computational studies, as well as the present study. Grimes performed some of the first such calculations of noble gas defects in UO_2 with classical potentials.[53] Our DFT + U results are in qualitative agreement with Grimes for the incorporation energy of noble gas atoms into octahedral sites, shown in Table IV. As the noble gas size increases, the energy to incorporate the atom increases. However, in contrast to DFT + U, Grimes found that helium has a negative incorporation energy in the interstitial site, meaning that helium energetically prefers to be in an interstitial rather than an isolated atom. For UO_2 to favorably incorporate helium into interstitial sites, there would have to be some favorable interaction between UO_2 and helium. Noble gas atoms does not have significant covalent or ionic chemical bonding with the UO_2, so another physical effect in the pair-potential model must be responsible: e.g., the attractive van der Waals force. For the van der Waals forces, Grimes used the Slater-Kirkwood formula, which is based on a gas phase dipole attraction. In the fluorite structure, the symmetry of the interstitial site does not allow a dipole to form; it only allows a multipole interaction that is inherently weaker and would give a larger equilibrium separation distance between the atoms than the dipole interaction. Hence, the classical potential used in Ref. 53 may overestimate the attractive force of a noble gas atom at an interstitial site. In addition, DFT has its own shortcomings: DFT does not capture van der Waals forces accurately,[52] so the incorporation energies reported here contain some error associated with this inaccuracy. We expect the errors to be small compared to the magnitude of the defect energies associated with noble gas impurities.

TABLE III. DFT + U calculated incorporation energies of interstitial noble gas atoms [Eq. (1)], formation energy of SD clusters [Eq. (2)], and solution energy of NG-SD complex defect complexes [Eq. (3)]. The strain associated with incorporating noble gas atoms into interstitial sites creates a large energetic penalty. The larger cavities created with the SDs alleviate some strain and reduce the energetic penalty of adding noble gas atoms.

Noble gas \ Defect type	Interstitial	SD1	SD2	SD3
	E (eV/defect cluster)			
	0	4.09	3.33	3.45
He	0.98	4.13	3.45	3.62
Ne	2.10	4.27	3.61	3.74
Ar	5.40	4.54	4.26	4.59
Kr	7.22	4.74	4.58	5.08
Xe	9.73	5.15	5.16	5.39

TABLE IV. Comparison of DFT + U and DFT (present work) with previous DFT and classical potential studies of incorporation energies of noble gas atoms into the interstitial site of UO_2 (eV/defect). Previous studies used classical potentials and various levels of DFT to calculate incorporation energies. FM, ferromagnetic; NM, nonmagnetic.

	Grimes (Ref. 53)	Freyss *et al.* (Ref. 10)	Petit *et al.* (Ref. 54)	Yun *et al.* (Ref. 12 and 42)	Geng *et al.* (Ref. 45)	Gryaznov *et al.* (Ref. 40)	Nerikar *et al.* (Ref. 32)	This work	
Method	Classical potentials	DFT (NM)	DFT	DFT	DFT + U	DFT + U	DFT + U	DFT (FM)	DFT + U
He	−0.13	−0.1	1.3	2.5		−0.25		1.08	0.98
Ne	4.62							2.39	2.10
Ar	9.83							6.04	5.40
Kr	13.31		14.2					8.06	7.26
Xe	17.23	11.2	19.0	1.43	9.75		11.11	11.19	9.73

Table V gives a comparison of solution energies of noble gas atoms into preexisting SDs in UO_2 from previous computational studies, as well as the present study. The literature values for incorporation energies of noble gas atoms into UO_2 given in Tables IV and V show a large amount of variation. Again, our DFT + U results give similar energetics for this quantity compared to the classical potential results of Grimes.[53]

Though our DFT + U results compare well with the classical potential works of Grimes, there are some surprising discrepancies with previous DFT results. Three of the previous DFT studies of noble gas atoms were not performed with DFT + U. Petit *et al.*[54] performed their calculations with LDA, Freyss *et al.* used PBE,[10] and Yun *et al.* used PW91.[12,42] These previous DFT calculations show a strong variation in incorporation energies and, as described previously, some surprising trends that are difficult to explain. For instance, the xenon incorporation energy calculated by Yun *et al.*[12,42] is smaller than the helium incorporation energy, despite the much larger size of xenon. This value of incorporation energy is different from all previous and current DFT and DFT + U results by ∼10 eV/defect or more. Our calculations do agree well with those of Geng *et al.*,[45] who used DFT + U, for the formation energy of xenon in an interstitial (within 20 meV). The solution energies [Eq. (3)] represented in Table V assume the SD cluster is preexisting in the lattice. The energy of helium incorporation into a SD1 in Ref. 54 and the xenon incorporation into a SD1 in Ref. 12 are negative and deviate largely from previous classical potential work of Grimes and our present DFT + U calcuations. A negative incorporation energy indicates that the energy of a noble gas atom in the SD is lower than a system with no defects. As mentioned previously, we expect noble gas atoms to have limited attractive interactions with the UO_2 host. Therefore, large, negative incorporation energies for noble gas atom should not occur. The discrepancies may be occur partly because previous DFT calculations neglect either magnetism, give a poor description of the electronic structure by using LDA/GGA (no U), or both. The strain energy due to a noble gas atom in a SD cluster changes based on the metallic/insulating nature of the material, and a proper description of DFT + U and magnetic structure is necessary to obtain the correct insulating state of UO_2. Because noble gas atoms do not interact with UO_2 with ionic or covalent bonding, the main interaction of noble gas atom is strain. The amount of strain caused by the noble gas atom varies with the volume of the cavity where it resides. And we showed earlier that the relative formation volume of a SD in metallic UO_2 (DFT no U) is negative while in insulating UO_2 (DFT + U) it is positive. This qualitative difference in the size of the SD affects the stain noble gas atoms impart and therefore the incorporation energy (see Fig. 4). It is unclear, though, why the authors of Ref. 10 would have found a negative incorporation energy.

Some studies of UO_2 do use DFT + U, but with mixed agreement with the present work. We suspect that some of these previous calculations may have converged to metastable electronic minima, even when the authors explicitly took these metastable states into consideration. While the agreement with Geng *et al.*[31] is good for xenon in an interstitial, we

TABLE V. Comparison of DFT + U and DFT (present work) with previous DFT and classical potential studies of solution energies of noble gas atoms into the preexisting SD clusters in UO_2 (eV/defect). There is good agreement between this work and the classical potentials of Grimes. The range of energies from previous DFT results is difficult to explain.

	Grimes (Ref. 53)	Petit *et al.* (Ref. 54)[a]	Yun *et al.* (Ref. 12)	Geng *et al.* (Ref. 45)	Nerikar *et al.* (Ref. 32)	This work	
Method	Classical potentials	DFT	DFT	DFT	DFT + U	DFT (no U) (SD1)	DFT + U (SD1)
He	−0.08	−6.0 to −5.9				0.19	0.04
Ne	0.13					0.35	0.19
Ar	0.67					0.94	0.45
Kr	1.09	1.4 to 2.2				1.26	0.66
Xe	1.16		−10.97	0.18	1.38	1.81	1.06

[a]Range represents energies for different SD clusters.

have very different energetics for xenon in a preexisting SD (1.06 vs 0.18 eV). However, we have good agreement for the incorporation energy of Xe–SD. Geng *et al*. find $\Delta E^{\text{Inc.}}_{\text{Xe-SD}}$ is 5.17 eV, while in the present work, we find $\Delta E^{\text{Inc.}}_{\text{Xe-SD}}$ is 5.19 eV. This comparison indicates that there must be disagreement between our calculations and those of Geng *et al*. for the SD cluster. Geng *et al*. find ΔE^{f}_{SD} is 4.99 eV, while we find $\Delta E^{\text{Inc.}}_{\text{Xe-SD}}$ is 4.09 eV. It is possible that the SD cluster calculation of Geng *et al*. was trapped in a higher-energy orbital occupation compared to our results. Nerikar *et al*.[32] found the incorporation energy to be >1 eV larger than our calculations for xenon. They found $\Delta E^{\text{Inc.}}_{\text{Xe-SD}}$ to be 3.88 eV and $\Delta E^{\text{Sol.}}_{\text{Xe-SD}}$ to be 1.38 eV. Both values are slightly lower than the present calculations. It is not clear whether the authors attempted to account for metastable orbital occupations in their calculations. If not, the reference state of bulk UO_2 could have an artificially high energy, thereby causing the defects to have artificially lower energy. Gryaznov *et al*.[30] calculated the incorporation of helium into the interstitial position using a small supercell of 25 atoms. They found that helium has a negative incorporation energy, which we suggest could be due to the small supercell size or metastable orbital occupations.

V. CONCLUSIONS

We have performed a series of DFT + U calculations to explore the energetics of various defects in UO_2, including noble gases (He, Ne, Ar, Kr, Xe), SDs, and combinations of these defects. We found that DFT + U is critical for accurate defect energetics. DFT + U, in addition to correctly describing the electronic structure of UO_2 as insulating, also qualitatively changes the formation volume of SD clusters in UO_2 (without U, this volume is negative, but including U the volume is positive). This volume change affects the incorporation energy of noble gas atoms into SDs. Distortions in the oxygen sublattice are observed experimentally and in DFT + U calculations that include noncollinear antiferromagnetism. However, we also found these distortions occur (but are symmetry lowering) in collinear AFM calculations. With this accurate (DFT + U, collinear AFM) description of UO_2, we calculated defect energetics. We found that the geometry of the SD results from a competition between electrostatic and surface energy effects. We calculated energetics of incorporating noble gas atoms into an interstitial site and found that the defect energy has a strong dependence on the volume of the noble gas atom, corresponding to the strain it causes in the interstitial site, from He (0.98 eV) to Xe (9.73 eV). When the noble gas atoms are incorporated in SDs, there is a strong favorable binding energy, due to strain relief associated with moving the noble gas atom from the highly strained interstitial position into the vacant space of the SD. The binding energy from strain relief for argon, krypton, and xenon is so large that if one of these atoms were in an interstitial position, it would be energetically favorable to form a SD to relieve the strain, thus making the critical nucleus of a xenon bubble, a single atom.

ACKNOWLEDGMENT

The authors acknowledge funding from the US Department of Energy under NERI-C Grant No. DE-FG07-07ID14893.

APPENDIX

$$\begin{pmatrix} 0.5 & 0.0 & 0.0 & 0.3 & 0.2 & 0.0 & 0.3 \\ 0.0 & 0.1 & 0.0 & 0.0 & 0.0 & 0.0 & 0.0 \\ 0.0 & 0.0 & 0.5 & -0.1 & 0.4 & -0.1 & -0.3 \\ 0.3 & 0.0 & -0.1 & 0.3 & 0.1 & 0.0 & 0.3 \\ 0.2 & 0.0 & 0.4 & 0.1 & 0.5 & -0.1 & -0.1 \\ 0.0 & 0.0 & -0.1 & 0.0 & -0.1 & 0.0 & 0.0 \\ 0.3 & 0.0 & -0.3 & 0.3 & -0.1 & 0.0 & 0.4 \end{pmatrix}$$

Orbital occupation matrix of pure UO_2 with oxygen distortions achieved using the U-ramping method of Ref. 29. This orbital occupation matrix differs from the one presented in Ref. 40.

*alexanderthompson2008@u.northwestern.edu

[1] A. F. Kohan, G. Ceder, D. Morgan, and C. G. Van de Walle, Phys. Rev. B **61**, 15019 (2000).
[2] C. Domain and C. S. Becquart, Phys. Rev. B **65**, 024103 (2001).
[3] C. G. Van de Walle and J. Neugebauer, J. Appl. Phys. **95**, 3851 (2004).
[4] D. Shin and C. Wolverton, Scr. Mater. **63**, 680 (2010).
[5] W. A. Counts, C. Wolverton, and R. Gibala, Acta Mater. **58**, 4730 (2010).
[6] F. Zhou and V. Ozolins, Phys. Rev. B **80**, 125127 (2009).
[7] P. Tiwary, A. van de Walle, and N. Grønbech-Jensen, Phys. Rev. B **80**, 174302 (2009).
[8] P. Tiwary, A. van de Walle, B. Jeon, and N. Grønbech-Jensen, Phys. Rev. B **83**, 094104 (2011).
[9] B. E. Hanken, C. R. Stanek, N. Grønbech-Jensen, and M. Asta, Phys. Rev. B **84**, 085131 (2011).
[10] M. Freyss, N. Vergnet, and T. Petit, J. Nucl. Mater. **352**, 144 (2006).
[11] T. Petit, in *Fission Gas Behaviour in Water Reactor Fuels* (OECD Publishing, Cadarache, France, 2002), p. 269.
[12] Y. Yun, H. Kim, H. Kim, and K. Park, J. Nucl. Mater. **378**, 40 (2008).
[13] Y. Yun, O. Eriksson, and P. M. Oppeneer, J. Nucl. Mater. **385**, 510 (2009).
[14] Y. Yun, O. Eriksson, P. M. Oppeneer, H. Kim, and K. Park, J. Nucl. Mater. **385**, 364 (2009).
[15] B. Jeon, M. Asta, S. M. Valone, and N. Grønbech-Jensen, Nucl. Instrum. Meth. B **268**, 2688 (2010).
[16] R. W. Grimes and C. R. A. Catlow, Phil. Trans. Roy. Soc. Lond. A **335**, 609 (1991).
[17] K. Govers, S. Lemehov, M. Hou, and M. Verwerft, J. Nucl. Mater. **366**, 161 (2007).

[18]K. Govers, S. Lemehov, M. Hou, and M. Verwerft, J. Nucl. Mater. **376**, 66 (2008).
[19]K. Govers, S. E. Lemehov, and M. Verwerft, J. Nucl. Mater. **405**, 252 (2010).
[20]J. Faber and G. H. Lander, Phys. Rev. B **14**, 1151 (1976).
[21]R. Laskowski, G. K. H. Madsen, P. Blaha, and K. Schwarz, Phys. Rev. B **69**, 140408 (2004).
[22]K. Ikushima, S. Tsutsui, Y. Haga, H. Yasuoka, R. E. Walstedt, N. M. Masaki, A. Nakamura, S. Nasu, and Y. Onuski, Phys. Rev. B **63**, 104404 (2001).
[23]Q. Yin and S. Y. Savrasov, Phys. Rev. Lett. **100**, 225504 (2008).
[24]S. L. Dudarev, D. N. Manh, and A. P. Sutton, Philos. Mag. B **75**(5), 613 (1997).
[25]A. I. Liechtenstein, V. I. Anisimov, and J. Zaanen, Phys. Rev. B **52**, R5467 (1995).
[26]L. Petit, A. Svane, Z. Szotek, W. M. Temmerman, and G. M. Stocks, Phys. Rev. B **81**, 045108 (2010).
[27]I. D. Prodan, G. E. Scuseria, and R. L. Martin, Phys. Rev. B **76**, 033101 (2007).
[28]K. N. Kudin, G. E. Scuseria, and R. L. Martin, Phys. Rev. Lett. **89**, 266402 (2002).
[29]B. Meredig, A. Thompson, H. A. Hansen, C. Wolverton, and A. van de Walle, Phys. Rev. B **82**, 195128 (2010).
[30]D. Gryaznov, E. Heifets, and E. Kotomin, Phys. Chem. Chem. Phys. **11**, 7241 (2009).
[31]H. Y. Geng, Y. Chen, Y. Kaneta, and M. Kinoshita, Phys. Rev. B **75**, 054111 (2007).
[32]P. V. Nerikar, X.-Y. Liu, B. P. Uberuaga, C. R. Stanek, S. R. Phillpot, and S. B. Sinnott, J. Phys. Condens. Matter **21**, 435602 (2009).
[33]G. Kresse and J. Hafner, Phys. Rev. B **47**, 558 (1993).
[34]G. Kresse, Ph.D. Thesis, Technische Universität Wien, Vienna, Austria, 1993.
[35]G. Kresse and J. Furthmüller, Comput. Mater. Sci. **6**, 15 (1996).
[36]G. Kresse and J. Furthmüller, Phys. Rev. B **54**, 11169 (1996).
[37]J. P. Perdew, in *Electronic Structure of Solids '91*, edited by P. Ziesche and H. Eschrig (Akademie Verlag, Berlin, 1991), p. 11.
[38]S. L. Dudarev, G. A. Botton, S. Y. Savrasov, C. J. Humphreys, and A. P. Sutton, Phys. Rev. B **57**, 1505 (1998).
[39]S. H. Vosko, L. Wilk, and M. Nusair, Can. J. Phys. **58**, 1200 (1980).
[40]B. Dorado, B. Amadon, M. Freyss, and M. Bertolus, Phys. Rev. B **79**, 235125 (2009).
[41]Y. Yun, P. M. Oppeneer, H. Kim, and K. Park, Acta Mater. **57**, 1655 (2009).
[42]Y. Yun, O. Eriksson, and P. M. Oppeneer, J. Nucl. Mater. **385**, 72 (2009).
[43]B. Dorado, G. Jomard, M. Freyss, and M. Bertolus, Phys. Rev. B **82**, 035114 (2010).
[44]F. Gupta, G. Brillant, and A. Pasturel, Philos. Mag. **87**(17), 2561 (2007).
[45]H. Y. Geng, Y. Chen, Y. Kaneta, M. Kinoshita, and Q. Wu, Phys. Rev. B **82**, 094106 (2010).
[46]S. L. Dudarev, M. R. Castell, G. A. Botton, S. Y. Savrasov, C. Muggelberg, G. A. D. Briggs, A. P. Sutton, and D. T. Goddard, Micron **31**, 363 (2000).
[47]F. Zhou and V. Ozolins, Phys. Rev. B **83**, 085106 (2011).
[48]Z. D. Popovic, J. P. Carbotte, and G. R. Piercy, J. Phys. F **4**, 351 (1974).
[49]M. W. Finnis, J. Phys. F **7**, 1999 (1977).
[50]M. J. Puska, S. Pöykkö, M. Pesola, and R. M. Nieminen, Phys. Rev. B **58**, 1318 (1998).
[51]A. E. Hughes and D. Pooley, *Real Solids and Radiation* (Wykeham Publications, London, 1975).
[52]W. Kohn, Y. Meir, and D. E. Makarov, Phys. Rev. Lett. **80**, 4153 (1998).
[53]R. W. Grimes, in *Fundamental Aspects of Inert Gases in Solids*, edited by Steve E. Donnelly and John H. Evans (Springer, New York, New York, 1990), p. 415.
[54]T. Petit, M. Freyss, P. Garcia, P. Martin, M. Ripert, J.-P. Crocombette, and F. Jollet, J. Nucl. Mater. **320**, 133 (2003).